



# Research and Application of Effective Exploitation Mechanism of Microscopic Pores in Heavy Oil Based on Displacement Pressure Gradient

Tingli Li\*, Jie Tan, Zhiqian Yuan

CNOOC (China) Co., Ltd. Tianjin Branch, Tianjin, China

\*Litl@cnooc.com.cn

**Abstract.** It is of great significance to study the effective exploitation mechanism of the micro-pores of heavy oil and design the corresponding injection and production pattern for enhanced oil recovery. Based on CT digital core technology, a lattice Boltzmann micropore simulation model was established to study the micropore displacement mechanism and oil displacement efficiency under different displacement pressure gradients. The results show that with the displacement pressure difference increasing from 0.3MPa to more than 0.8MPa, the medium and small pore crude oil with pore throat radius less than 80 $\mu$ m gradually begins to flow. As the viscosity of crude oil increases from 80mPa·s to 260mPa·s, the flow resistance of crude oil in medium and small pores increases sharply, and the displacement pressure gradient increases to more than 0.008MPa/m, which is conducive to improving the flow capacity of crude oil in medium and small pores, thus greatly improving the overall displacement efficiency. The above knowledge is applied to the development of QHD heavy oil field in Bohai Sea during the high water cut period. The strategy of large-scale utilization of horizontal well joint directional well development adjustment is adopted, and the anti-nine-point well pattern is adjusted from the initial directional well to the five-point well pattern of horizontal well joint directional well. The oil production rate is increased from 0.8% to 1.5% ~ 2.1%, and the water cut rise rate is controlled at about 0.6%. Water drive recovery rate increased from 24.5% to 39.3%, which greatly improved the development effect and provided experience for similar oil fields.

**Keywords:** heavy oil, displacement characteristics, displacement pressure gradient, horizontal well, development strategy.

## 1 Introduction

The continental sandstone heavy oil field in Bohai Sea is dominated by delta and fluvial facies deposits. The reservoirs are characterized with an average porosity of 35% and an average permeability of 3600mD, and the formation oil viscosity is 50 ~ 450mPa·s. With the deepening of oilfield development, the high water cut stage presents the char

recovery. It is urgent to explore the characteristics of continental heavy oil displacement and carry out the corresponding injection and production pattern adjustment to improve the development effect in the high water cut stage. At present, the research on the micro-displacement characteristics of heavy oil mainly focuses on the micro-seepage mechanism, reservoir change characteristics and the distribution of remaining oil, but there are few studies on the formation mechanism and effective use of micro-pore remaining oil<sup>[1-2]</sup>.

In view of the above situation, based on CT digital core technology, a lattice Boltzmann micro-pore simulation model for water flooding was established to study the micro-pore displacement mechanism, displacement rule and effective displacement pressure gradient of different pore throat radii, so as to guide the adjustment of injection and production well pattern in high water cut period, in order to improve the oilfield development effect.

## 2 Oil-water two-phase microscopic pore network model

### 2.1 Micro-pore mesh modeling based on CT technology

Firstly, the core plunger is de-oiling, de-salting, drying, volume rendering, mirror processing, etc., and then the core is sliced. Nano-ct scanning and high-resolution microscopic image processing technology are used to conduct scanning imaging with X-ray absorption characteristics, reflecting the fine characteristics of the target object, and a higher resolution core slice is obtained. In order to effectively reduce the impact of noise on skeleton boundary recognition during CT scan slicing, grayscale image denoising processing means of mean filter and median filter are used to obtain grayscale image stack, and threshold values are selected to binarize grayscale images, and pore connectivity is appropriately adjusted to reflect and describe core pore microstructure. Such as pore shape, size, distribution and connectivity. Finally, the pore and rock skeleton are extracted to obtain the effective pore spatial distribution that can reflect the characteristics of the actual reservoir, and thus a microscopic network model reflecting the real pore structure of the core is constructed (FIG. 1).

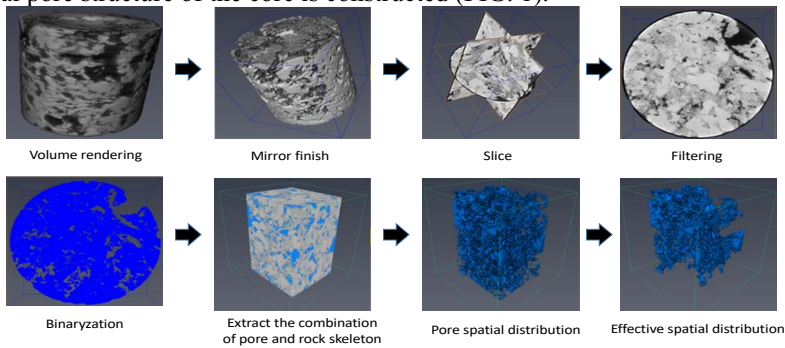


**Fig. 1.** Pore grid modeling process

## 2.2 Lattice Boltzmann micro-simulation method for water flooding

The lattice Boltzmann method can describe the microscopic fluid interaction and complex geometric boundaries, and is widely used in digital core porous media flow simulation. It is mainly composed of discrete velocity model, equilibrium distribution function and distribution function evolution equation.

Using the lattice Boltzmann D2Q9 model, the discrete velocity model expression is as follows:

$$e_i = \begin{cases} (0,0), & i = 0 \\ c \left( \cos \left[ (i-1) \frac{\pi}{2} \right], \sin \left[ (i-1) \frac{\pi}{2} \right] \right) & i = 1,2,3,4 \\ \sqrt{2}c \left( \cos \left[ (2i-1) \frac{\pi}{4} \right], \sin \left[ (2i-1) \frac{\pi}{4} \right] \right) & i = 5,6,7,8 \end{cases} \quad (1)$$

In formula (1),  $e_i$  is the velocity in direction  $i$ ;  $i$  represents the discrete velocity direction of the D2Q9 model, respectively 0,1,2, ..., 8 directions;  $c$  is the unit cell speed, that is, the ratio of the cell step to the time step.

Bhatnagar et al. proposed a lattice Boltzmann equation<sup>[3-8]</sup> based on the simplified collision term of Boltzmann equation. The model expression is as follows:

$$f_i^\sigma(\mathbf{r} + e_i \delta_t, t + \delta_t) - f_i^\sigma(\mathbf{r}, t) = -\frac{1}{\tau} \left[ f_i^\sigma(\mathbf{r}, t) - f_i^{\sigma(eq)}(\mathbf{r}, t) \right] + \overline{F}_i^\sigma(x, t) \quad (2)$$

In equation (2),  $f_i^\sigma$  is the density distribution function of the particle in the  $i$  direction,  $r$  is the spatial position of the fluid particle,  $t$  is the time,  $\tau$  is the relaxation time,  $\delta_t$  is the time step. In equation (2), the expression of the external force term  $\overline{F}_i^\sigma(r, t)$  is:

$$\overline{F}_i^\sigma(r, t) = \frac{F^\sigma \cdot (e_i - u_\sigma^{eq})}{\rho_\sigma c^2} f_i^{\sigma(eq)} \quad (3)$$

In formula (3),  $F^\sigma$  is the sum of the forces acting on the component  $\sigma$ , including the two-phase fluid force, the fluid-rock force, and the displacement pressure.

The expression of equilibrium distribution function of particles  $f_i^{\sigma(eq)}$  in each direction is as follows:

$$f_i^{\sigma(eq)} = \rho_\sigma \omega_i \left[ 1 + 3(e_i \cdot u_\sigma^{eq}) + \frac{9}{2}(e_i \cdot u_\sigma^{eq})^2 - \frac{3}{2}(u_\sigma^{eq})^2 \right] \quad (4)$$

In formula (4),  $\sigma$  represents the oil phase or the water phase, and the weight coefficient is expressed as:

$$\omega_i = \begin{cases} 4/9, & i = 0 \\ 1/9, & i = 1,2,3,4 \\ 1/36, & i = 5,6,7,8 \end{cases} \quad (5)$$

The expressions of the fluid macroscopic density  $\rho_\sigma$  and velocity  $u_\sigma$  are respectively:

$$\rho_\sigma = \sum_i f_i^\sigma \quad (6)$$

$$u_\sigma = \left( \frac{1}{\rho_\sigma} \sum_i f_i^\sigma e_i + \frac{\delta_t}{2} F^\sigma \right) \quad (7)$$

In this paper, from the microscopic perspective of molecular dynamics, the continuous fluid is dispersed into a large number of continuous microscopic particle clusters, and the particle cluster movement is decomposed into collision steps and migration steps, and the particle clusters migrate to adjacent nodes after completing the collision step at a certain node, and then calculate the macroscopic physical quantities such as density and velocity according to the new particle distribution function, so as to realize the microscopic pore water flooding simulation.

### 3 Mechanism and rule of effective displacement in microscopic pores

#### 3.1 Effective displacement mechanism of microscopic pores

Firstly, a simulation study with a crude oil viscosity of  $120\text{mPa}\cdot\text{s}$  and a displacement pressure gradient of  $0.008\text{MPa/m}$  was carried out to obtain the oil-water two-phase velocity field (calculated with a time step of  $\delta t=54000$ ), as shown in FIG. 2. It can be seen that in the initial state, the non-wetting phase (oil phase) filled the entire pore and distributed in a contiguous state. At the beginning of displacement, the wetting phase (water phase) first rapidly flows to displace the oil phase along the macropores along the main stream line. Then, with the progress of displacement, the water phase gradually enters the middle pores connected with the macropores and some small pores, and the spread range of the water phase gradually expands, forming a large continuous distribution, while the oil phase is gradually displaced out. At the end of displacement, the crude oil in the large pores on the main stream line was completely driven out by water, and the crude oil in the middle pores directly connected with the large pores and some small pores were also driven out by water phase. The water flooding swept in the pores far away from the main stream line was less, and most of the crude oil remained<sup>[9-10]</sup>.

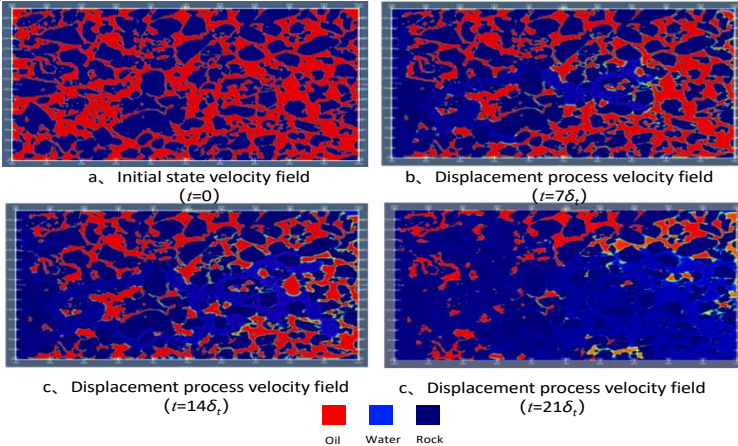


Fig. 2. Microscopic pore displacement process

### 3.2 Effective displacement rule of microscopic pores

Further study on the relationship between oil displacement efficiency and displacement pressure gradient of crude oil with viscosity of 80mPa·s, 170mPa·s and 260mPa·s, as shown in FIG. 3, it can be seen that the displacement efficiency of crude oil with different viscosity increases to different degrees with the increase of displacement pressure gradient. Low viscosity oil can achieve a higher displacement efficiency of 61.2% under a smaller displacement pressure gradient of 0.005MPa, medium viscosity oil can achieve a higher displacement efficiency of 60.3% only when the displacement pressure gradient increases to 0.008MPa, and high viscosity oil can achieve a higher displacement efficiency of 45.5% only when the displacement pressure gradient increases to 0.012MPa. This shows that with the increase of crude oil viscosity, the force between crude oil particles and rock particles in porous media increases rapidly, and the flow resistance of crude oil increases sharply. The smaller the pore radius is, the larger the seepage resistance will be with the increase of crude oil viscosity. In particular, the force between crude oil particles and rock particles in medium and small pores with pore throat radius less than 80nm increases more significantly.

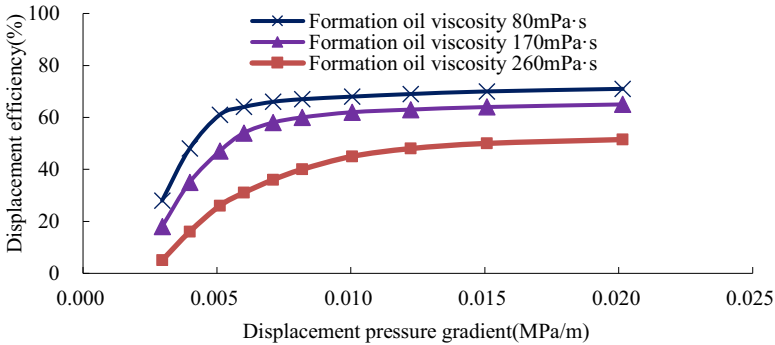


Fig. 3. Relationship between displacement efficiency and displacement pressure gradient

## 4 Oilfield application

QHD oilfield is the first large fluvial heavy oil field of 100 million tons in Bohai Sea. At the beginning, the directional well pattern was reversed and the injection-production well spacing was 350m. In the high water cut period, the strategy of stratified development and adjustment of horizontal Wells combined with directional Wells was adopted, and 124 horizontal Wells were adjusted from the reverse nine-point pattern of directional Wells to the five-point pattern of horizontal Wells combined with directional Wells (FIG. 4, 5), and the injection-production well distance was adjusted from 350m to 220m. After the adjustment, the displacement pressure gradient is increased from 0.004MPa/m to 0.085MPa/m, the displacement efficiency is increased from 35.6% to 58.6%, the oil recovery rate is increased from 0.8% to 2.1%, the water drive recovery rate is increased from 24.5% to 35.6%. It has become a typical oil field for efficient development in ultra-high water cut period offshore.

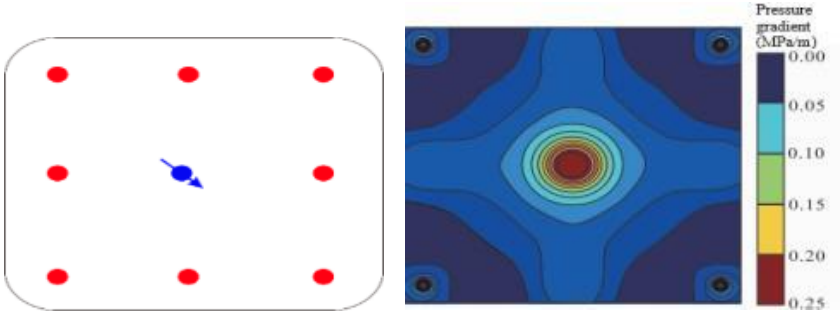


Fig. 4. Initial development mode of QHD Oilfield

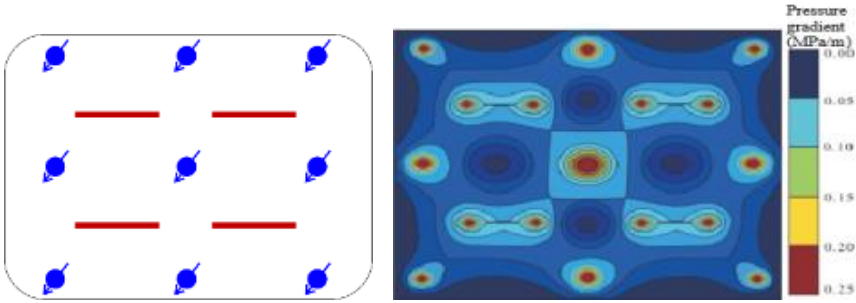


Fig. 5. Development mode of QHD oilfield after well pattern adjustment

## 5 Conclusion

The micro-simulation method was used to reveal the displacement mechanism and rule of micro-pores. The flow resistance of crude oil in micro-pores increased with the decrease of pore throat radius and the increase of crude oil viscosity. The displacement pressure gradient increased to more than 0.008MPa/m, which was conducive to improving the flow ability of medium and small pore oil with pore throat radius less than 80nm. In the high water cut period of QHD oilfield in Bohai Sea, the development mode of horizontal well combined directional well stratified system is adopted to greatly improve the water drive recovery efficiency and further develop and enrich the theory of efficient development of continental heavy oil fields.

## References

1. Jia Z W, Yuan M, ZHANG X L: Waterflooding microscopic flow characteristics and the remained oil starting mechanisms. *Petroleum Geology & Oilfield Development in Daqing*, 37(1): 65-70(2018).
2. KANG Y M, LI M, WANG L G: Microscopic waterflooding percolation characteristics of Yan8 Formation in Block S1, Yanwu Oilfield, Ordos Basin. *Petroleum Geology and Recovery Efficiency*, 26(5): 48-57 (2019).

3. Hill R J, Koch D L, Land A J C: The first effects of fluid inertia on flow in ordered and random arrays of spheres. *Journal of Fluid Mechanics*, 448,213(2001).
4. Chai Z, Shi B, Lu J, et al: Non-Darcy flow in disordered porous media:a lattice Boltzmann study .*Computers & Fluids* ,39(10), 2069(2010).
5. Jonas T: Implementation of a lattice Boltzmann kernel using the compute unified device architecture developed by nVIDIA. *Computing and Visualization in Science*,13(1), 29 - 39(2010).
6. Pan C X, Prins J F, Miller C T: A high-performance lattice Boltzmann implementation to model flow in porous media. *Computer Physics Communications*, 158,89 - 105(2004).
7. Obrecht C, Kuznik F, Tourancheau B: A new approach to the lattice Boltzmann method for graphics processing units. *Computers & Mathematics with Applications*,61(12) ,3628 - 3638(2011).
8. Zhu L H, Guo Z L: GPU accelerated lattice Boltzmann simulation of flow in porous media. *Chinese Journal of Computational Physics*,32(1),20-26(2015).
9. Zhou Z L, Cai M J, Zhang F L: Occurrence state and time-lapse characteristics of remaining oil after multi-media flooding in high water-cut reservoirs. *Fault Block Oil and Gas Fields*, 27(05): 608-612(2020).
10. Li J L, Liu Y, Gao Y J: Effects of microscopic pore structure heterogeneity on the distribution and morphology of remaining oil. *Petroleum Exploration and Development*, 45(6): 1043-1052(2018).

**Open Access** This chapter is licensed under the terms of the Creative Commons Attribution-NonCommercial 4.0 International License (<http://creativecommons.org/licenses/by-nc/4.0/>), which permits any noncommercial use, sharing, adaptation, distribution and reproduction in any medium or format, as long as you give appropriate credit to the original author(s) and the source, provide a link to the Creative Commons license and indicate if changes were made.

The images or other third party material in this chapter are included in the chapter's Creative Commons license, unless indicated otherwise in a credit line to the material. If material is not included in the chapter's Creative Commons license and your intended use is not permitted by statutory regulation or exceeds the permitted use, you will need to obtain permission directly from the copyright holder.

